

# Investigation of water droplet impingement under conditions of the secondary cooling zone of a continuous caster

Lukas Preuler<sup>1</sup>, Mario Peyha<sup>2</sup>, Christian Weiß<sup>2</sup>, Christian Bernhard<sup>2</sup>, Sergiu Ilie<sup>3</sup>

<sup>1</sup>K1-MET GmbH  
Stahlstrasse 14, Austria, 4020-Linz  
Phone: +43 38424022237  
Email: lukas.preuler@k1-met.com

<sup>2</sup>Montanuniversitaet Leoben  
Franz-Josef-Strasse 18, Austria, 8700-Leoben  
Phone: +43 3842 402 5009  
Email: mario-kurt.peyha@stud.unileoben.ac.at  
Email: christian.weiss@unileoben.ac.at  
Email: christian.bernhard@unileoben.ac.at

<sup>3</sup>voestalpine Stahl GmbH  
voestalpine-Strasse 3, Austria, 4020-Linz  
Phone: +43 50304158690  
Email: sergiu.ilie@voestalpine.com

Keywords: continuous casting, secondary cooling, spray properties, water droplet impingement

## ABSTRACT

Optimal cooling strategies for the secondary cooling zone of the continuous casting process are crucial for the production of high-quality steel slabs. To find such strategies it is necessary to understand the influence of spray properties on the cooling performance. Our experimental set-up allows a comparative monitoring of water droplet impingement characteristics on cold and hot steel surfaces. Droplet sizes and velocities at different air-mist spray conditions were examined by laser diffraction analysis and high-speed imaging. Partly, discrimination between incoming primary spray and secondary droplets formed during splashing could be achieved. For all experiments, the area of spray overlapping was of special interest.

## INTRODUCTION

In the secondary cooling zone (SCZ) of the continuous casting process 40 – 90 % of the heat is removed from the slab. A major part of the cooling is achieved by spray cooling, using water or air-mist nozzles. On the one side, the cooling performance has to be sufficient to ensure shell growth and the complete solidification of the material. On the other side, uniform and smooth cooling characteristics are important to avoid crack propagation or crack formation. To meet these conditions a fundamental understanding of spray properties is crucial. The impingement of water droplets on the steel surface is influenced by the size and the velocity of the droplets. In addition to water impact, the temperature on the surface is important, since above Leidenfrost-temperature a stable vapor film between surface and spray water is formed.<sup>[1] [2] [3] [4]</sup>

Several researchers investigated the properties of air-mist sprays with a variety of measuring methods. Flores et.al.<sup>[5]</sup> for example used a particle droplet image analyzer to determine droplet size and velocity of a single air-mist spray. A high-speed camera was used to record droplet impingement at surface temperatures between 500 and 1200 °C. Ramstorfer and Chimani<sup>[6]</sup> chose a 2D-Phase-Doppler-Anemometer to determine droplet size and velocity in air-mist sprays. Lorenzetto and Lefebvre<sup>[7]</sup> have investigated the droplet size of a plain-jet atomizer. In this work the droplet size and droplet velocity of air-mist sprays at certain air/water flow ratios are measured. The influence of spray overlapping and the droplet impingement on a cold and hot surface are investigated using two cooling nozzles.

## EXPERIMENTAL METHODS

All experiments were performed inside the Nozzle Measuring Stand (NMS), which was developed at the Chair of Iron and Steel Metallurgy, Montanuniversitaet Leoben. The main purpose of the NMS is the characterization of one or two cooling

nozzles in terms of water distribution (WD) and heat transfer coefficient (HTC).<sup>[8]</sup> To measure the droplet properties the methods of laser diffraction analysis and high-speed camera measurement were added to the experimental set-up. This was done with the support of the Chair of Process Technology and Industrial Environmental Protection, Montanuniversitaet Leoben. In the SCZ of a continuous slab caster, it is common to mount several nozzles next to each other in order to cool the complete width of the strand. Uniform cooling can be ensured by spray overlapping. To show the influence of overlapping, experiments were performed with one and two nozzles. Figure 1 describes the used nozzle layout with the two measurement points P1 and P2. The distance between the nozzles ( $N_x$ ) and the distance from the surface to the nozzle tip ( $N_z$ ) can be adjusted to change the cooling performance.

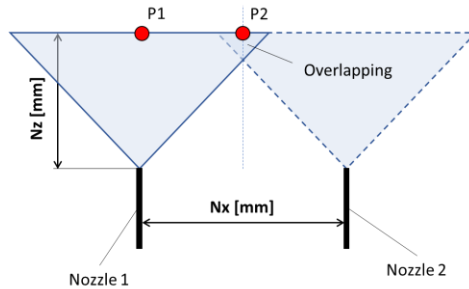


Figure 1. Nozzle layout

Besides the nozzle layout, also the nozzle operation parameters can be varied. To show the impact of distance and water/air flow rates on the spray properties, the parameter specifications from Table 1 were used. An important value for the evaluation of the experimental results is the ratio of air to water flow, short A/W-ratio.

Table 1. Overview on used nozzle operation parameters

$N_z$ - $N_x$	$V(H_2O)$	$p(H_2O)$	$V(AIR)$	$p(AIR)$	A/W
mm-mm	l/min	bar	$l_n$ /min	bar	$l_n/l$
205-528	9.35	2.5	94	1.3	10
	4.5	1.3	163	1.3	36
271-700	4.5	1.8	233	2	52

### Laser diffraction analysis

For the determination of the water droplet size, the NMS was extended by the method of laser diffraction analysis, schematically shown in Figure 2a. The used device (Sympatec, Helos Vario KF Magic) consists of an emitter and a receiver, which are both mounted to a moving unit to change the position of measurement. A laser beam moves from the emitter through the air-mist spray (measuring zone) where it interacts with single water droplets. Along the optical path beyond the measuring zone, a lens is focusing the scattered light to the center of a detector plate. The radial intensity characteristic of the detected light pattern correlates with the size of the water droplet.<sup>[9] [10]</sup>

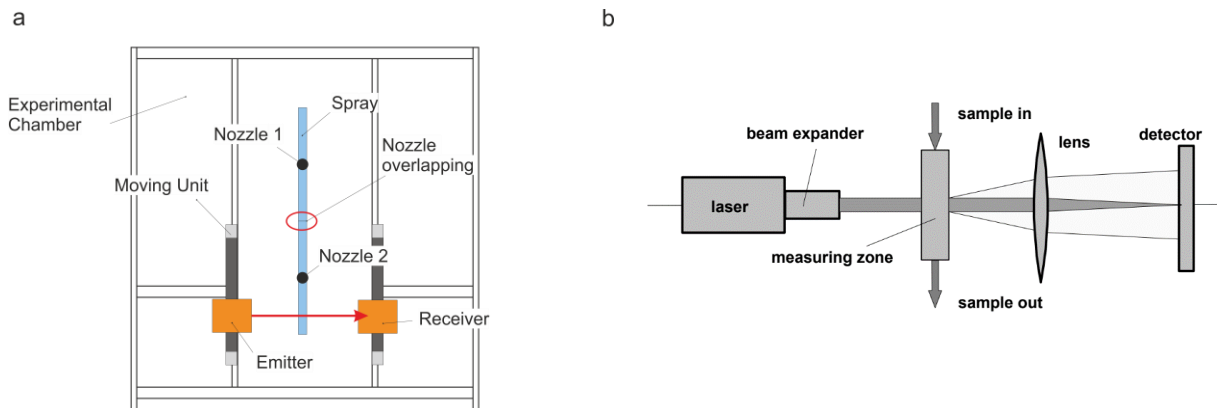


Figure 2. a) Experimental set-up for laser diffraction analysis; b) Detail of measurement principle<sup>[9]</sup>

With each parameter specification, 10 measurements were performed to enable statistical evaluation. The processing of the measured data was done by Sympatec software. Figure 3 shows an example of the droplet size distribution  $Q_3$  and the frequency distribution  $q_3$  for two A/W-ratios. For further comparison between the parameter set-ups it was decided to use the mass median diameter,  $d_{50}$ .

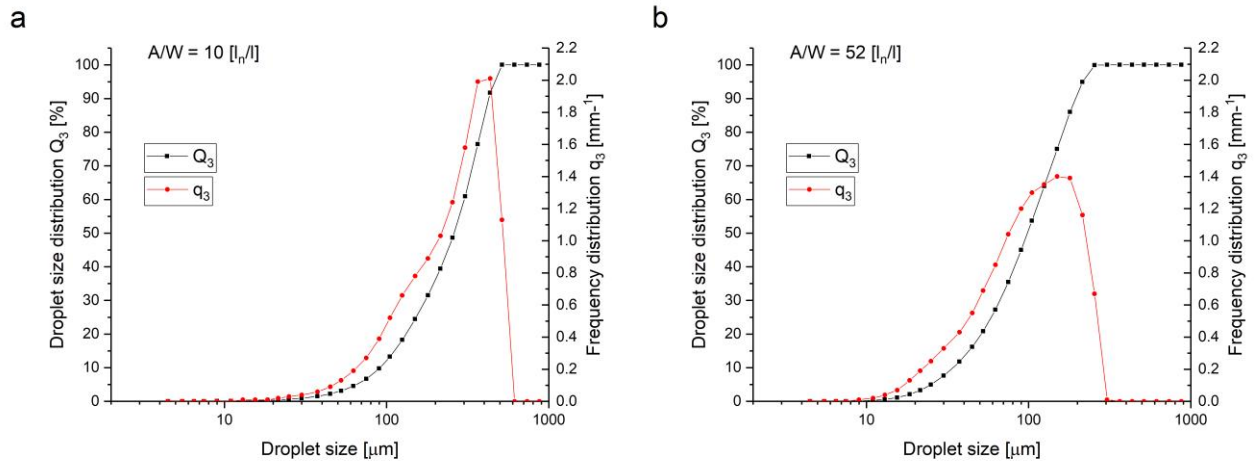


Figure 3. Droplet size distribution  $Q_3$  and frequency distribution  $q_3$  for A/W ratios of a)  $10 \text{ l}_n/\text{l}$  and b)  $52 \text{ l}_n/\text{l}$

### Shadow imaging

For the investigation of droplet velocity and the phenomenon of droplet impingement on cold and hot surfaces, the method of shadowgraphy was used. Figure 4a shows the developed experimental set-up in which one or two nozzles are mounted inside the experimental chamber of the NMS. On one side, a high power LED-spotlight is attached to the structure, which illuminates the droplets of the air-mist spray. A high-speed camera (LaVision, IMAGER PRO HS 4M) is located on the opposite side, protected from the spray water. The optical magnification is realized by using a long distance microscope with a depth of field of about 0.6 mm. The shadow of every droplet, which moves through the focused spray section, is captured by the camera. For the impingement experiments the chosen spray section has a size of approximately 6 mm x 6 mm and the recording rate is set to about 9850 frames per second (fps). The measurement of the droplet velocity is done with 11470 fps for the same spray section size. Before the actual measurement starts, the nozzle tip is covered by a deflection sheet. The cover is removed after the defined operation parameters are reached. This procedure enables the investigation of the initial phase of droplet impingement and reduces the amount of mist inside the chamber, what increases measurement accuracy. Another action to enhance visibility is the use of a spray separator as described in Figure 4b. The spray separator consists of two symmetrically positioned knife edges, which form a small central gap and remove the off-axis fraction of the spray liquid.

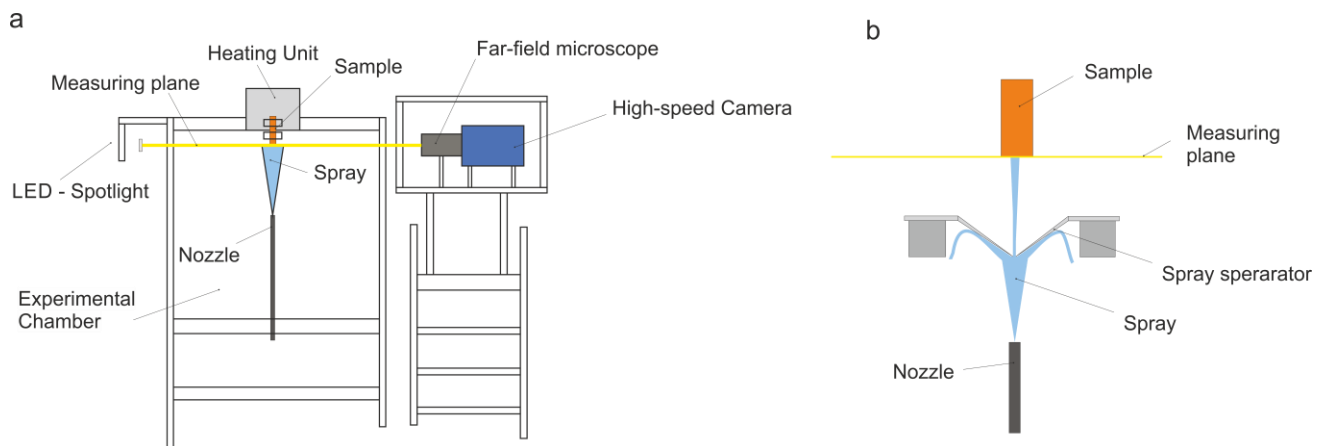


Figure 4. (a) Experimental set-up and (b) spray separator

The total recording time for each measurement was about 35 ms. The gained data was divided into four packages, starting with the moment of first droplet appearance. This enables to investigate the evolution of droplet velocity over measurement time. The evaluation of each data package was done by an in-house Matlab program. The program divides the visible droplets into

several diameter classes (50 – 100  $\mu\text{m}$ , 100 – 150  $\mu\text{m}$ , 150 – 200  $\mu\text{m}$ , 200 – 300  $\mu\text{m}$  and 300 – 500  $\mu\text{m}$ ) and calculates their velocity by comparing their position over time. For further comparison, a mean droplet velocity over all diameter classes and data packages was calculated. For the visualization of the recordings, a color code from light to dark blue was chosen. The darker the area the higher the optical density in measuring direction. This means that areas containing water appear in dark blue, areas containing mostly air in light blue.

## RESULTS

The data sets were evaluated in terms of averaged spray properties like mean droplet size and ensemble averaged droplet velocity, interaction mechanism between two sprays and the impingement on hot and cold surfaces.

### Primary spray properties

Figure 5 compares the droplet size and velocity for certain A/W-ratios and distances at measurement point P1. The experiments have shown, that the spray properties strongly depend on the A/W-ratio. The bigger the A/W-ratio, the smaller and the faster the droplets. The distance between the nozzle and the measurement plane has almost no impact on the droplet size, but on the velocity. A change of this distance from 205 to 271 mm leads to a reduction of the droplet velocity of about 40-60 % at P1. Smaller droplets decelerate faster due to higher frictional force.<sup>[11]</sup>

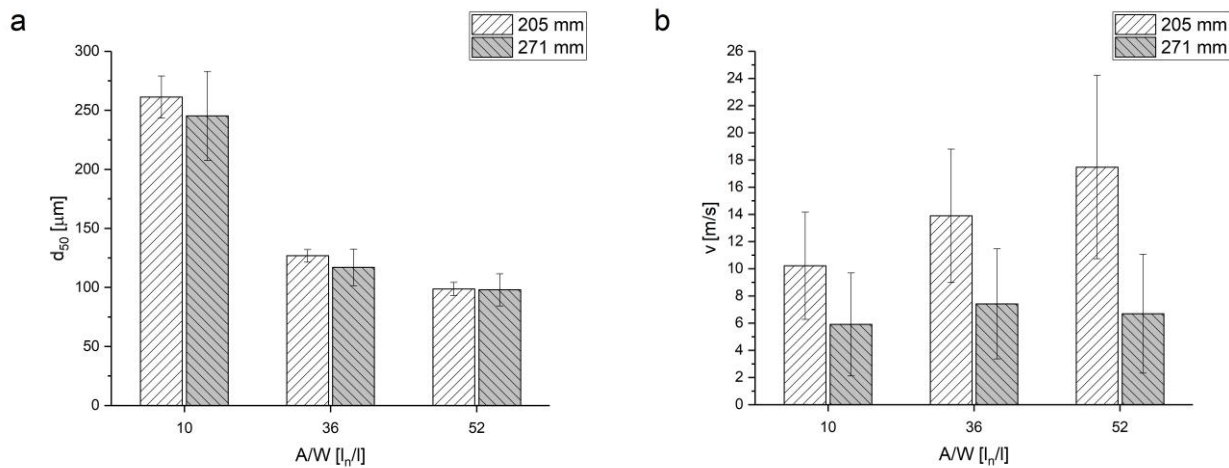


Figure 5. Measurement point P1, a) Mean droplet size and b) ensemble averaged droplet velocity for different A/W-ratios and nozzle-measuring plane distances ( $N_z$ ).

### Spray interaction

The overlapping of air-mist sprays leads to interaction phenomena, which have influence on droplet size and velocity. If two nozzles are operated, droplets from both air-mist sprays collide what results in more, smaller droplets. An example for a droplet collision is shown in Figure 6.

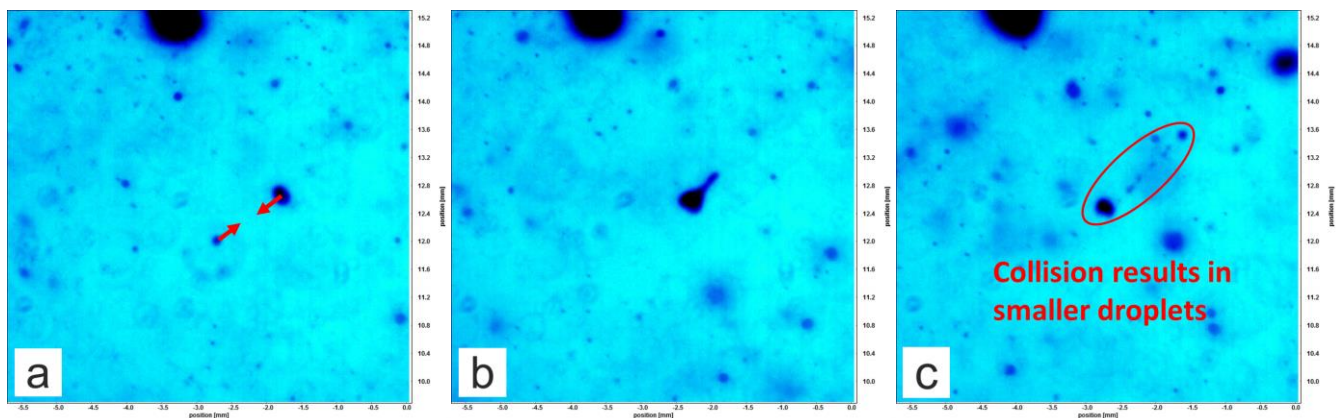


Figure 6. Example for droplet collision in the region of spray cone overlapping; (a) before, (b) during and (c) after the collision

The frequency of collision strongly depends on the size of the droplets. The bigger the droplet size, the higher the probability of collision.<sup>[12]</sup> This is confirmed by Figure 7, where the measured droplet size from one and two nozzle experiments at point P2 is compared. The operation of two nozzles reduces the resulting droplet velocity. Smaller droplets are again more affected because of the higher frictional force.<sup>[11]</sup>

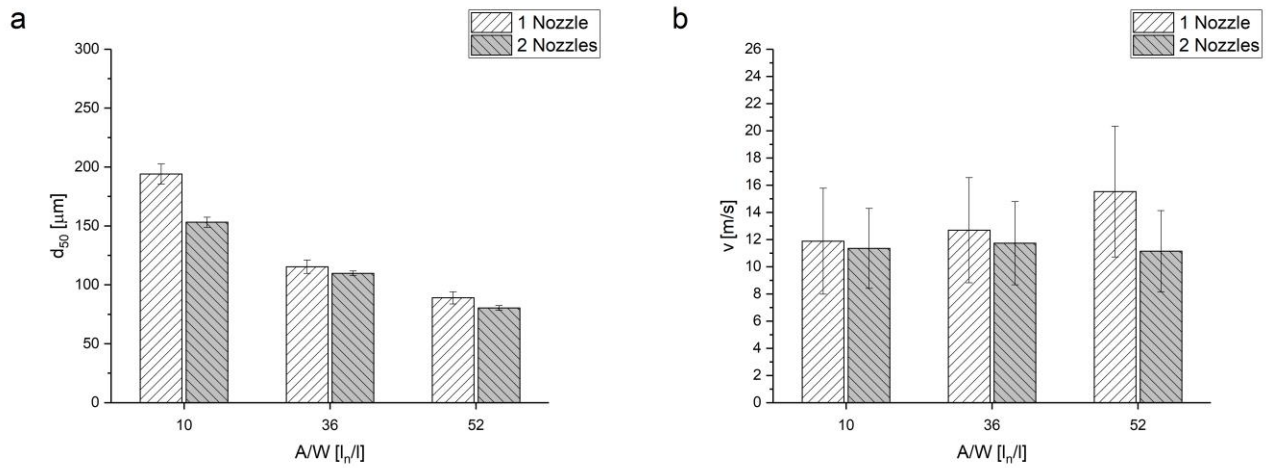


Figure 7. Influence of spray overlapping on a) droplet size and b) droplet velocity at  $Nz = 205$  mm.

### Spray impingement

For the investigation of droplet impingement, a sample made of austenitic steel was mounted inside the NMS. How droplets react after impinging on a surface mainly depends on the surface temperature and the Weber ( $We$ ) number. To consider first one, experiments with cold ( $20\text{ }^\circ\text{C}$ ) and hot ( $1000\text{ }^\circ\text{C}$ ) samples were performed. Water impingement at surface temperatures above the so-called Leidenfrost-temperature leads to the formation of a vapor-layer, which has significant influence on the droplet behavior and the cooling performance. The  $We$ -number is calculated according to Equation 1. The dimensionless number gives the ratio between kinetic energy and surface energy of a particle.<sup>[1][2]</sup>

$$We = \frac{\rho_{H2O} \cdot v_d^2 \cdot d_d}{\sigma_{H2O}} \quad (1)$$

The droplet velocity  $v_d$  and diameter  $d_d$  are determined by experiments. The density  $\rho_{H2O}$  and the surface tension  $\sigma_{H2O}$  of water at  $20\text{ }^\circ\text{C}$  and  $100\text{ }^\circ\text{C}$  are taken from literature.<sup>[13]</sup> All used operation parameters result in a  $We$ -number bigger than 100. Figure 8 describes that in case of high  $We$ -numbers and surface temperatures above Leidenfrost-temperature the phenomenon of splashing is expected. The primary droplet impinges on the surface, where it comes to the formation of vapor. The vaporization results in a layer of smaller secondary droplets, that are moving over the surface. In case of a surface temperature of  $20\text{ }^\circ\text{C}$  and unchanged  $We$ -number the droplet impingement results in the formation of a water film and some secondary droplets splashing away from the surface.<sup>[1]</sup>

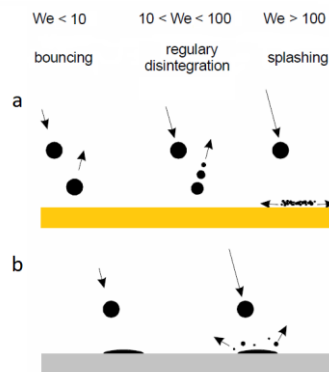


Figure 8. Phenomenon of droplet impingement at a) surface temperature at  $1000\text{ }^\circ\text{C}$  (above Leidenfrost-temperature) and b) at  $20\text{ }^\circ\text{C}$  <sup>[1]</sup>

Figure 9 shows the recorded surface impingement on the cold surface after a spray duration of 5 ms. At this point, the spray properties are still evolving and no stationary experimental conditions are not yet reached. Droplets hit the surface and the splashing process occurs as marked in Figure 9a. A dense film of water starts to form while secondary droplets move away from the surface. Recordings of water impingement on the heated surface are presented in Figure 10 and again the process of splashing is confirmed. In this case, droplets reach the surface and form a layer of very fine secondary droplets mixed with vapor.

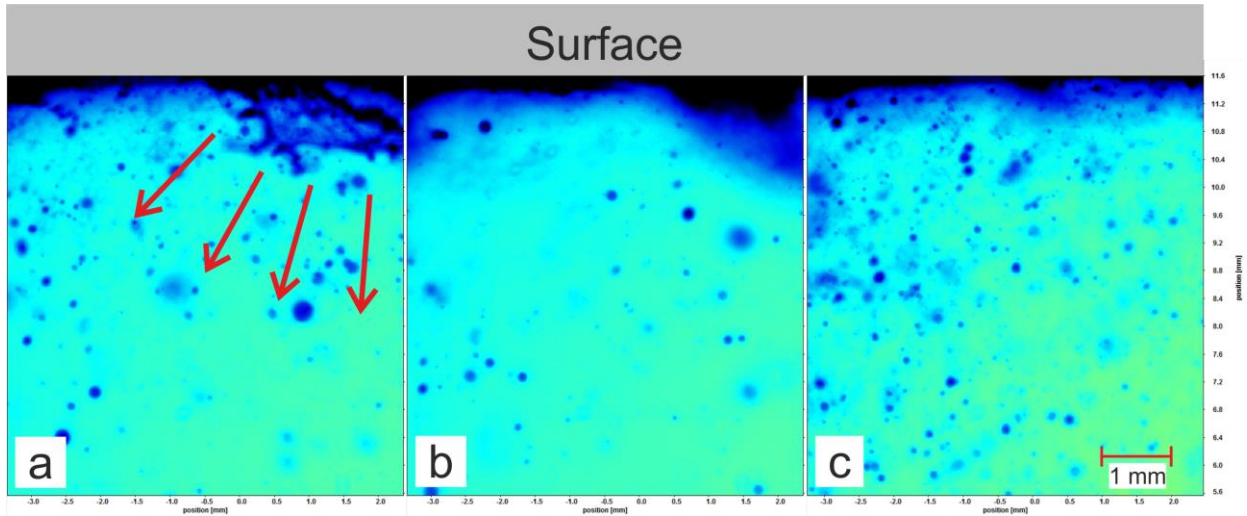


Figure 9. Droplet impingement at P2, 1 Nozzle,  $T_s = 20\text{ °C}$ ,  $t = 5\text{ ms}$ , A/W-ratio of a) 10, b) 36 and c) 52  $l_n/l$

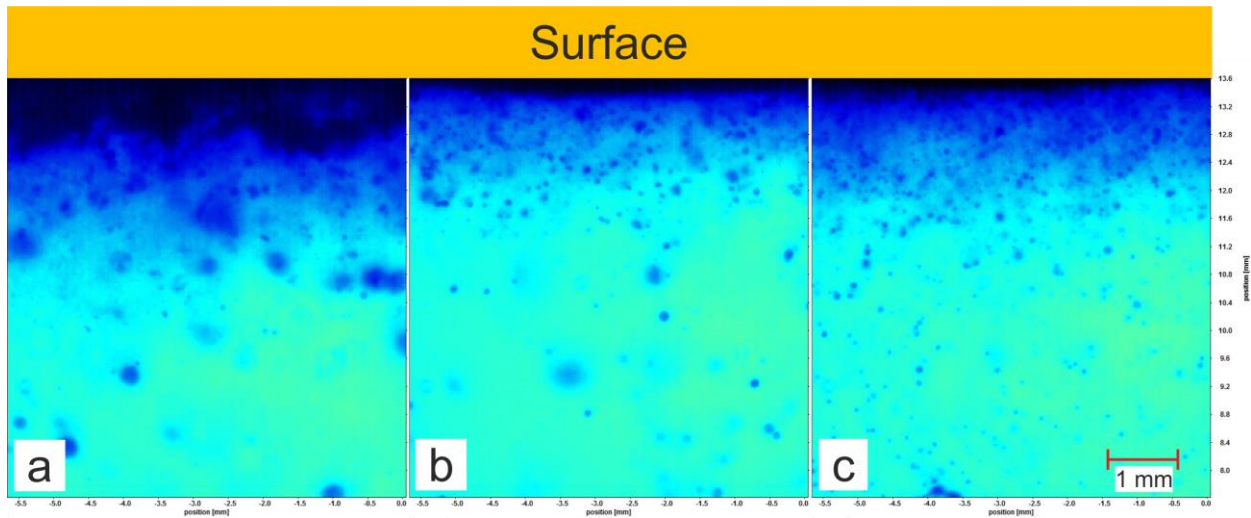


Figure 10. Droplet impingement at P2, 1 Nozzle,  $T_s = 1000\text{ °C}$ ,  $t = 5\text{ ms}$ , A/W-ratio of a) 10, b) 36 and c) 52  $l_n/l$

After a period of 20 ms no further change in the water impingement process is observed; a stationary experimental condition is established. Figure 11 shows, that on the cold surface the thickness of the water film depends on the amount of water flux and therefore on the A/W-ratio. The lower the A/W-ratio the thicker the surface water film. If a droplet impinges on the water film, a water crown is formed. [14] [15] It is assumed, that the wall tangential velocity induced by the primary air-mist spray applies a shear force onto the crown and this shear force leads to asymmetric emission of secondary droplets from the disintegrating crown crest. In Figure 11b, some secondary droplets and the direction of their movements are marked. Impingement on the heated surfaces is displayed in Figure 12. The thickness of the formed layer is increasing with increasing A/W-ratio. An explanation for this behavior could be the lower droplet size for higher A/W-ratios and the higher amount of mist in the surrounding area.

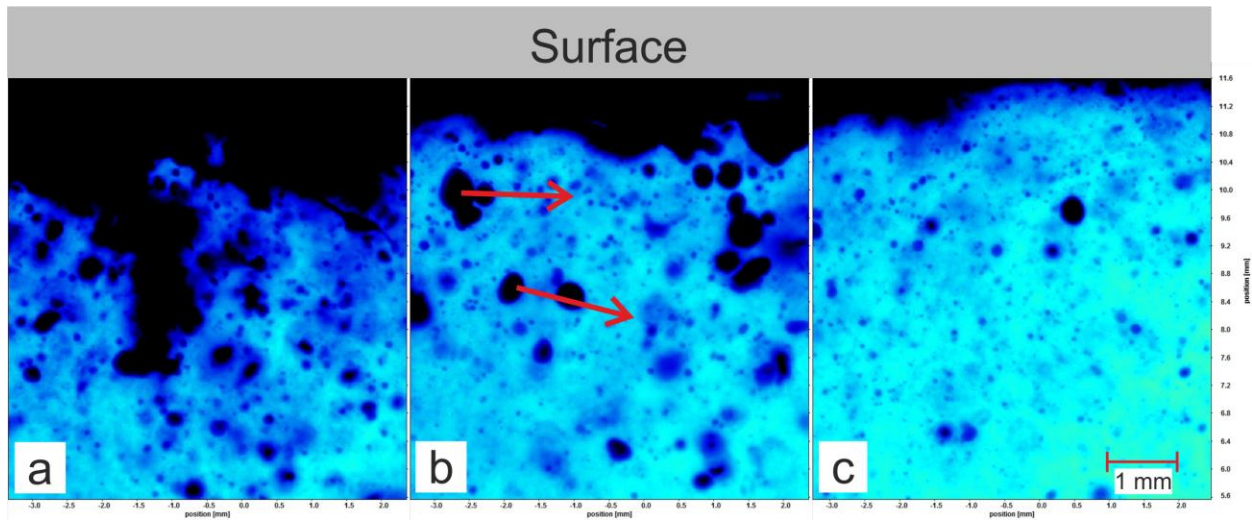


Figure 11. Droplet impingement at P2, 1 Nozzle,  $T_s = 20\text{ }^\circ\text{C}$ ,  $t = 20\text{ ms}$ , A/W-ratio of a) 10, b) 36 and c) 52  $l_n/l$

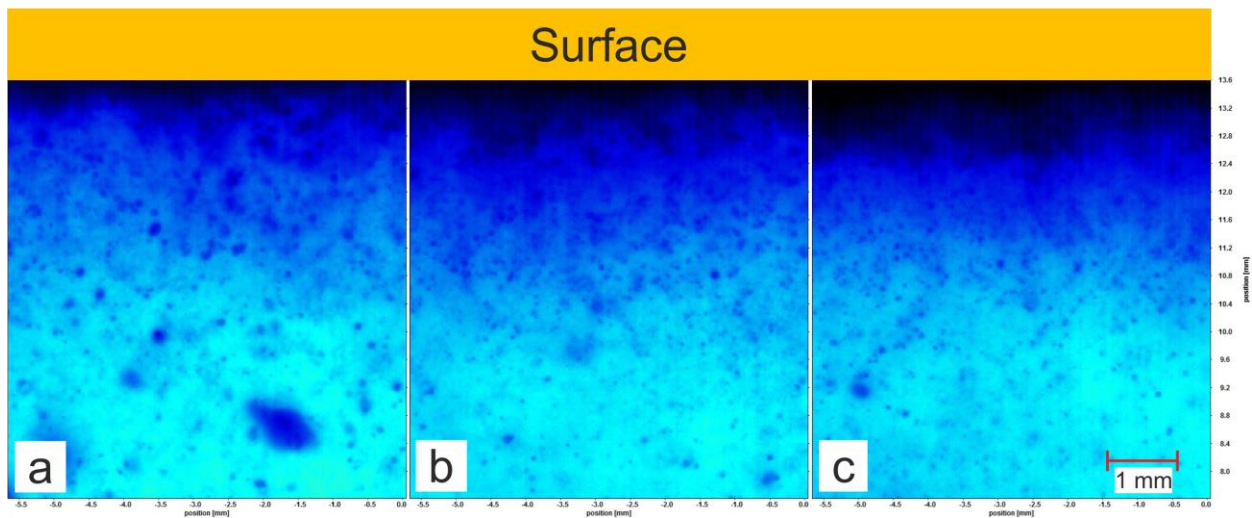


Figure 12. Droplet impingement at P2, 1 Nozzle,  $T_s = 1000\text{ }^\circ\text{C}$ ,  $t = 20\text{ ms}$ , A/W-ratio of a) 10, b) 36 and c) 52  $l_n/l$

The difference between experiments with one and two nozzles is shown in Figure 13. In case of two nozzles, the dense layer close to the hot surface is thicker. A possible explanation could be the higher amount of water and the smaller overall droplet size in the interaction region.

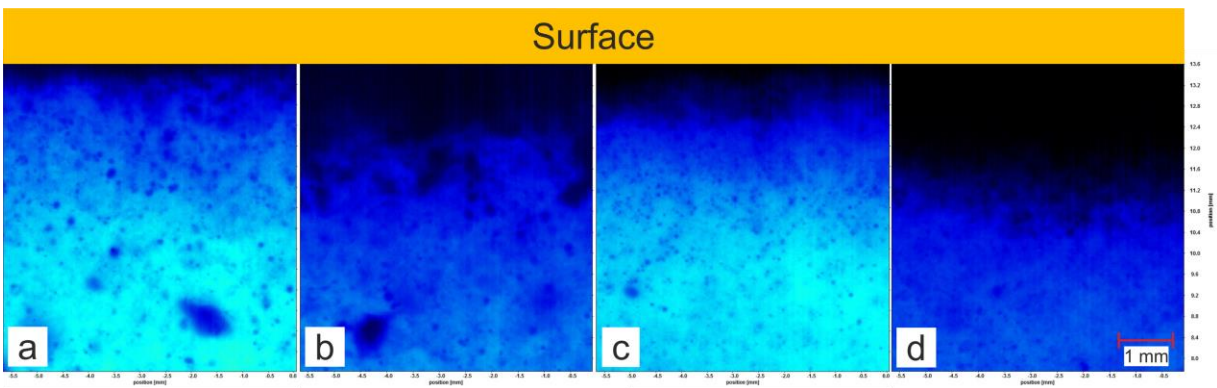


Figure 13. Droplet impingement at P2,  $T_s=1000\text{ }^\circ\text{C}$ ,  $t=20\text{ ms}$ , (a) A/W=10  $l_n/l$ , 1 Nozzle, (b) A/W=10  $l_n/l$ , 2 Nozzles, (c) A/W=52  $l_n/l$ , 1 Nozzles, (d) A/W=52  $l_n/l$ , 2 Nozzles

## DISCUSSION

Before the nozzle operation parameters were reached and the shadow imaging measurements started, the nozzles were covered by a deflection sheet to reduce the amount of mist in the experimental chamber. For the two nozzle experiments the simultaneous removal of the cover from both nozzles is crucial to ensure correct measurement conditions.

The droplet size was determined with both experimental methods, laser diffraction analysis and shadow imaging. Figure 14a shows a comparison of measured droplet size at position P1 and Figure 5b at position P2. In both cases the trend is the same; the droplet size is decreasing with increasing A/W-ratio. However, the estimated  $d_{50}$  values show differences between 5 and 87 %. Due to a higher statistical significance, it was decided to use the mean droplet size measured by laser diffraction analysis.

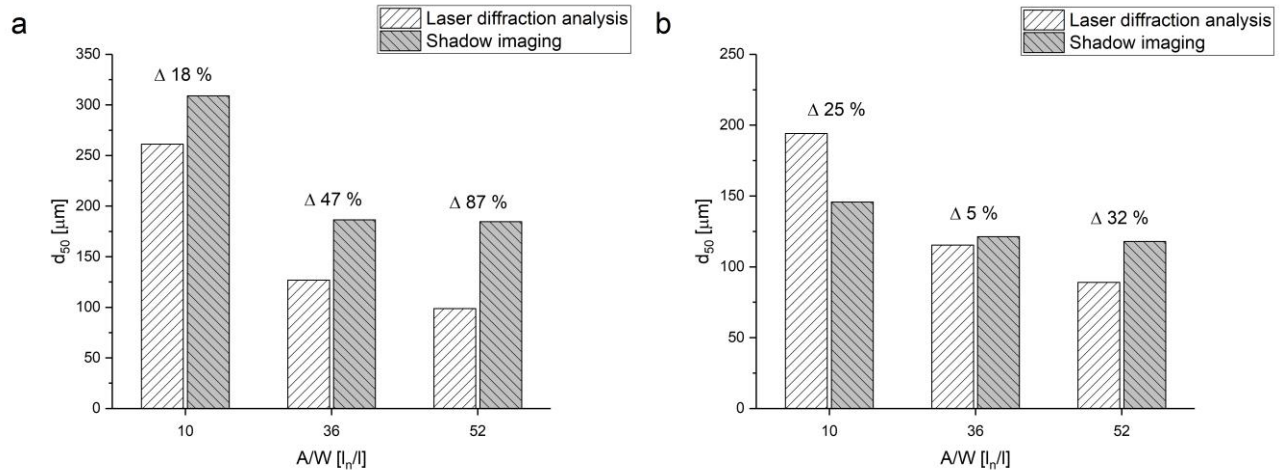


Figure 14. Mean droplet size measured by laser diffraction analysis and shadow imaging ( $N_z = 205$  mm, 1 Nozzle) at measurement position (a) P1 and (b) P2

## CONCLUSION

In this work, methods for the measurement of water droplet size and velocity in air-mist sprays were examined. Applying these experimental methods in combination with variations of nozzle operation parameters, nozzle distance and number of operated nozzles following conclusions could be made:

- Mean droplet size of primary spray is decreasing with increasing A/W-ratio.
- Averaged droplet velocity of primary spray is increasing with increasing A/W-ratio.
- A change of distance between nozzle tip and measurement plane has no significant influence on mean droplet size but reduces the averaged droplet velocity of the primary spray.
- Spray cone overlapping leads to a reduction of mean droplet size and averaged droplet velocity.
- The process of splashing for We-numbers  $> 100$  and surface temperatures of  $20$  °C and  $1000$  °C was confirmed.
- Droplet impingement on cold surfaces results in the formation of water surface films and the formation of secondary droplets. The lower the A/W-ratio the thicker the water film.
- Droplet impingement above Leidenfrost-temperature leads to a layer of fine secondary droplets. The thickness of the layer increases with higher A/W-ratios as well as spray cone overlapping.

## REFERENCES

1. F. Puschmann, Dissertation: Experimentelle Untersuchung der Spraykühlung zur Qualitätsverbesserung durch definierte Einstellung des Wärmeübergangs, *Otto-von-Guericke-Universität Magdeburg*, 2003
2. S.Nukiyama, The maximum and minimum values of the heat  $Q$  transmitted from metal to boiling water under atmospheric pressure, *Int. J. Heat Mass Transfer*, 27, 7, (1984), pp. 959-970
3. J. Sengupta, B.G. Thomas and M.A. Wells, The Use of Water Cooling during the Continuous Casting of Steel and Aluminum Alloys, *Metallurgical and Materials Transactions A*, 36A, (2005), pp. 187-204



4. K. Schwerdtfeger, Metallurgie des Stranggießens, *Verlag Stahleisen mbH*, Düsseldorf, Germany, (1992)
5. T. M. Flores F., A.H. Castillejos E. and B.G. Thomas, Heat Extraction and Droplet Impact Regimes Obtained with Continuous Casting Air-mist Nozzles, *AISTech 2017 Proceedings*, (2017), pp. 1751-1760
6. F. Ramstorfer and C. Chimani, Influence of air / water volume ratio on the spray cooling heat transfer coefficient of air-mist nozzles, *3<sup>rd</sup> International Conference on Simulation and Modelling of Metallurgical Process in Steelmaking Proceedings*, Leoben, (2009), pp. 1-6
7. G.E. Lorenzetto and A. H. Lefebvre, Measurements of Drop Size on a Plain-Jet Airblast Atomizer, *AIAA Journal*, 15, 7, (1977), pp. 1006-1010
8. L. Preuler, C. Bernhard, S. Ilie and J. Six, Experimental investigations on spray characteristics of water/air nozzles, *European Conference of Continuous Casting ECCO 2017*, (2017), pp. 19-27
9. S. Röthele and W. Witt, Laser Diffraction: Millenium-Link for Particle Size Analysis, *Powder Handling & Process*, 11, 1, (1999), pp. 1-11
10. G. Wozniak, Zerstäubungstechnik, *Springer-Verlag Berlin Heidelberg New York*, (2002), pp. 111-116
11. B.P. Husted, The physics behind water mist systems, *IWMA conference Rome*, (2004), pp. 1-15
12. C. Weiss, The liquid deposition fraction of sprays impinging vertical walls and flowing films, *International Journal of Multiphase Flow*, 31, (2005), pp. 115-140
13. W. Wagner and H.J. Kretschmar, International Steam Tables – Properties of Water and Steam based on the Industrial Formulation IAPWS-IF97, *Springer-Verlag Berlin Heidelberg*, (2008), p. 321
14. T.Y. Ma, F. Zhang, H.F. Liu and M.F. Yao, Modeling of droplet/wall interaction based on SPH method, *International Journal of Heat and Mass Transfer*, 105, (2017), pp. 296-304
15. T. Ma, L. Feng, H. Wang, H. Liu and M. Yao, A numerical study of spray/wall impingement based on droplet impact phenomenon, *International Journal of Heat and Mass Transfer*, 112, (2017), pp. 401-412